NON-LINEAR ELASTIC BEHAVIOR OF BITUMEN EMULSION STABILIZED MATERIALS WITH C&D WASTE AGGREGATES

B. Gómez-Meijide [a,*], *I. Pérez* [a]

[a]*Universidade da Coruña. E.T.S.I. Caminos, Canales y Puertos, Campus de Elviña s/n, 15071. A Coruña, Spain*

**Corresponding author. Tel.: +34-981167000. Fax: +34-981167170*

E-mail addresses: breixo.gomez.meijide@udc.es (B. Gómez Meijide), iperez@udc.es (I. Pérez)

Abstract

In this paper, the non-linear elastic behavior of bitumen stabilized materials with emulsion (BSM-E)[1] with recycled aggregates from construction and demolition (C&D)[2] waste was analyzed by means of dynamic triaxial tests. Different predicting models were fitted to the experimental resilient modulus; the Mohr-Coulomb envelopes were obtained, and the Huurman's model was fitted to experimental creep data to provide the necessary parameters for eventual numerical simulations. The results show that mixes with C&D aggregates are more flexible, have better resistance to permanent deformation and similar failure stress than mixes with natural aggregates. However, they needed a higher water and bitumen content.

Keywords

Bitumen stabilized materials with emulsion; construction and demolition waste; non-linear elastic behavior; resilient modulus; Mohr-Coulomb envelope; permanent deformation

Highlights

Non-linear elastic behavior of BSM-E with CDWA[3] was studied

Dynamic triaxial tests were conducted, treating BSM-E as granular materials

Resilient and creep models were fitted to the experimental results

Mohr-Coulomb envelopes were obtained

BSM-E with CDWA showed good properties but a need for greater bitumen content

---

[1] BSM-E: bitumen stabilized materials with emulsion
[2] C&D: Construction and Demolition
[3] CDWA: Construction and Demolition Waste Aggregates
[4] HMA: Hot Mix Asphalt
[5] NA: Natural Aggregates

1. Introduction

Bitumen stabilized materials with emulsion (BSM-E) are constituted of a mix of aggregates, asphalt emulsions and water at room temperature. This mixture does not require heating before mixing, what makes it more ecological and economical, especially compared with other sorts of asphalt mixes such as conventional hot mix asphalt (HMA)[4]. However, due to their trend to show higher air-void content after compaction and weak early life strength, the BSM-E were traditionally considered inferior to HMA [1], and their use was almost restricted to surface treatments and reinstatement work on low traffic roads and walkways [2,3,4,5]. Today, with the latest developments in cold asphalt technology, this trend is changing, and the BSM-Es are again gaining growing popularity within the scope of the fight against climate change in civil engineering [6, 7, 8].

BSM-Es, as materials featuring cold in-place recycling in road rehabilitation, are materials that combine the influence of all of their components to create a complex visco-elasto-plastic material with anisotropic characteristics. As Jenkins and Yu (2009) [9] describe, the matrix of these emulsion stabilized materials is "*neither fish nor fowl*", behaving similarly to both granular materials (stress dependency) and HMA (temperature and frequency of loading dependency).

Furthermore, according to Jenkins et al. (2007) [10] and Ebels (2008) [11], after their production, these materials show two different phases: the curing phase (6-18 months) with an increase in the initial stiffness due to the moisture reduction and densification, and the stiffness reduction phase with a new decrease in the stiffness. According to these authors, the non-linear elastic behavior (similar to granular materials and characterized by stress dependency [12]) tends to be highlighted during the first phase, whereas after curing, the visco-elasto-plastic behavior (similar to HMA and characterized by dependency on temperature and frequency of loading [13]) becomes more significant. The first behavior is best studied by means of triaxial tests (like unbound granular materials) and the latter can be assessed by the application of typical HMA tests, such as Indirect tensile Stiffness Modulus (ITSM) or Dynamic Modulus |E*| tests.

The environmental and even the economic aspects of BSM-E can be improved by substituting the natural aggregates (NA)[5] with recycled construction and demolition waste aggregates (CDWAs).

Table 1. Components of recycled aggregate (% of total dry weight)

Material	**% In Coarse Aggregate (12/24 mm)**	**% In Medium Aggregate (6/12 mm)**
Concrete and mortar	70%	55%
Natural aggregates	25%	40%
Ceramics and masonry materials	3.7%	4.1%
Concrete with metal pieces	1.121%	< 0.001%
Concrete with textile fibers	0.146%	0.042%
Plaster/gypsum	0.103%	0.012%
Other materials (metal, paper, plastic, glass)	< 0.1%	0.1%

Table 2. Characterization of recycled and natural aggregates

Property	**Specification**	**Recycled aggregate**	**Natural aggregate**
Flakiness Index	UNE EN 933-3 [24]	4.5%	19.8%
Crushed particles	UNE EN 933-5 [25]	89%	94%
Sand equivalent	UNE EN 933-8 [26]	77	78
Los Angeles coefficient	UNE EN 1097-2 [27]	38	14
Bulk specific gravity	UNE EN 1097-6 [28]	2.64 t/m^3	2.78 t/m^3
Dry specific gravity	UNE EN 1097-6 [28]	2.23 t/m^3	2.74 t/m^3
SSD specific gravity	UNE EN 1097-6 [28]	2.39 t/m^3	2.75 t/m^3
Absorption	UNE EN 1097-6 [28]	7.0%	0.5%

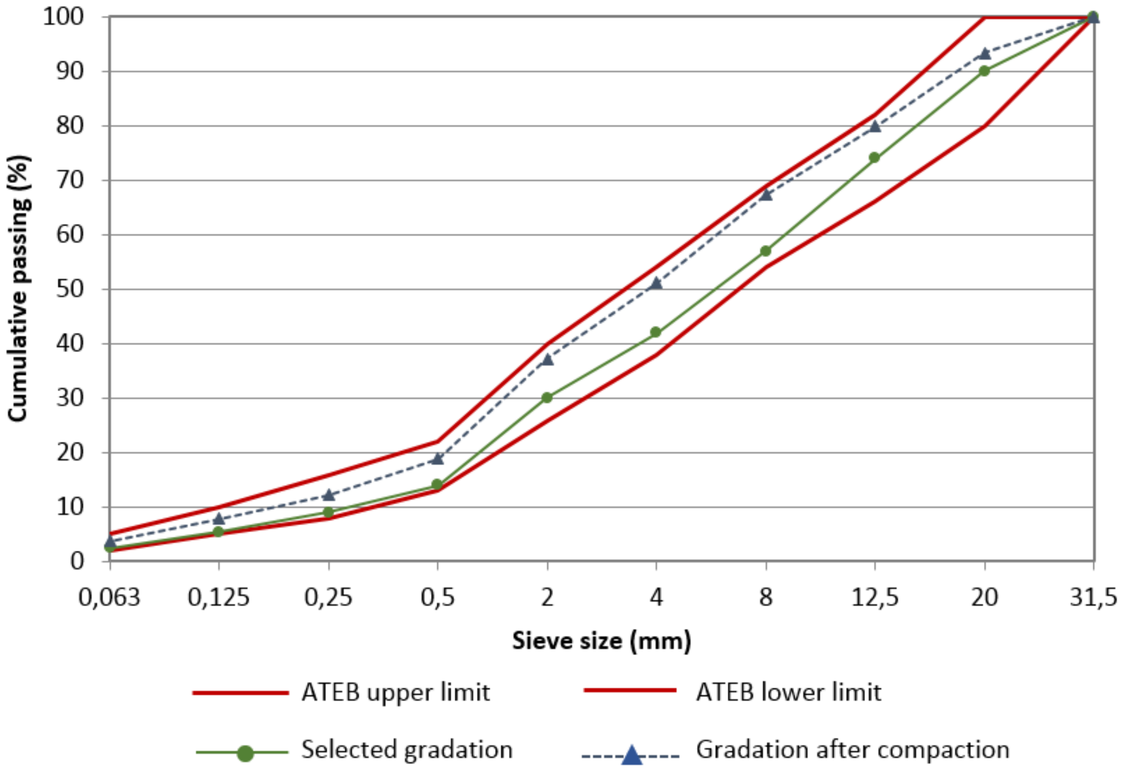

Figure 1. Aggregate gradation of CDWA before and after compaction compared with ATEB recommendations

This research area has already been studied and has demonstrated great success for other construction materials such as concrete [14, 15, 16] or HMA [17, 18, 19], and a study was also initiated for mixtures with asphalt emulsion [20, 21, 22].

Because the visco-elasto-plastic behavior of cured BSM-E with CDWA has already been studied in other publications [20, 21, 22], the aim of this investigation was to begin to understand the non-linear elastic behavior of these materials. For this purpose, BSM-Es before and after curing were treated as granular materials and studied by means of dynamic triaxial tests. Finally, three different predicting models for resilient modulus were fitted to the experimental results, the Mohr-Coulomb envelopes were obtained, and the Huurman's model [23] was fitted to experimental creep data to provide the necessary parameters for eventual numerical simulations.

2. Materials and preparation of specimens

The recycled aggregate was made from construction and demolition waste materials. Thus, the main part of this recycled aggregate was composed of concrete, mortar and stone, with a certain proportion of impurities such as ceramics, metal pieces, gypsum, plastics and glass (Table 1). The control mixes were made with hornfels, a common metamorphic siliceous NA extracted from a local quarry in Ourense (Spain). As Table 2 shows, the high absorption and low specific gravity of CDWA is especially noticeable.

The gradation limits were provided by the technical reports of the Spanish Technical Association of Bituminous Emulsions (ATEB) for GE1 grave-emulsions [29]. The amount of fine particles was adjusted to the lower limit because the amount of fine particles tends to increase after the mixing and compaction processes (Figure 1). This could be checked by means of chemical binder removal and resieving of samples that had already been compacted.

Finally, a cationic slow-setting bitumen emulsion (60% bitumen content) with 100 pen grade base bitumen was selected.

To assess how the bitumen and water content as well as the sort of aggregate affect the results, 12 different mixes (six with each kind of aggregate) were tested (Table 3). These combinations were chosen by varying only one parameter while keeping the others fixed. Water content refers to the initial amount of water present during the mixing process. As tested after compaction, the remaining water is much less and does not depending to any significant extent on the initial mixing content [21].

To meet the requirements of the Standard EN 13286-7 [30] (the diameter of specimens must be at least five times the maximum size of the aggregate, and the height must be twice the diameter), specimens were made by stacking two 101.6-mm-high samples. These 101.6-mm height x 101.6-mm diameter cylindrical specimens were produced according to the Standard NLT-161, somehow derived from the French *Duriez* test (NF P98-251) [31] and widely used for BSM-E in Spain. The mixes were subsequently compacted by means of a static load of 21 MPa for 2 min.

This production method, which involves the stacking of two samples, has already been used by other authors [13, 32] in purely compressive tests, certifying that the samples behave exactly like one-piece specimens.

To assess how the curing of the mixes affects the results, all of the tests were repeated with cured and uncured samples. The cured samples were obtained by subjecting the samples to a 3-day curing process in the oven at 50ºC, according to ATEB recommendations [29].

Table 3. Water and bitumen content of the mixes tested with CDWA and NA

CDW Aggregate				**Natural Aggregate**			
% Residual Bitumen	**% Water**			**% Residual Bitumen**	**% Water**		
	Mixing	**After Compaction**	**After Curing**		**Mixing**	**After Compaction**	**After Curing**
5%	**9%**	8.6%	3,2%	**2%**	**3%**	2,9%	0,1%
6%	**9%**	8.2%	3,5%	**3%**	**3%**	2.3%	0,1%
7%	**9%**	7,8%	3,8%	**4%**	**3%**	1,4%	0,2%
8%	**9%**	7,5%	4,0%	**5%**	**3%**	1,2%	0,4%
7%	**21%**	7,6%	3,8%	**4%**	**9%**	1,8%	0,2%
7%	**33%**	7,5%	3,7%	**4%**	**15%**	1,9%	0,4%

3. Resilient behavior

3.1 Dynamic triaxial test

The experimental results were obtained using a dynamic triaxial apparatus, composed of a removable chamber and the axial load system generator (Figure 2). The confining pressure was supplied by air, using an independent air compressor (maximum pressure 10 bar). The axial load generator was controlled by a hydraulic system.

The specimens were sealed with an elastic membrane fixed to the upper and lower plates with O-rings to prevent the entry of the confining air into the samples. Axial strain was measured with two LVDTs placed on the upper plate.

The tests were conducted at 20±2ºC with a constant confining pressure (CCP) and sinusoidal deviator stress, according to the Standard EN 13286-7 [30]. The stresses used in each sequence were selected according to the Standard for the top of the base layers, directly under the thin surface courses (less than to 80 mm). In addition to being the most unfavorable case, this arrangement typical where grave-emulsions are found.

The test involved first a 70 kPa conditioning confining stress (σ_3) and a cyclic axial deviator stress (σ_d), oscillating from 5 kPa to 340 kPa (minimum stress of 0 kPa was rejected to ensure the contact between specimen and actuator at any time) and at a frequency of 1 Hz. The conditioning was finished when one of the following criteria was met:

- The axial permanent strain regime started being lower than 10^{-7} per cycle
- The variation of the resilient modulus started being lower than 5 kPa per cycle
- The number of load cycles exceeded 20,000 cycles

Figure 2. Sample and sensor arrangement for the resilient modulus triaxial test according to the Standard EN 13286-7

Once the conditioning was finished, the test was conducted through 29 sequences with different σ_d-σ_3 combinations (Table 4). Due to the characteristics of the equipment, it was not feasible to produce cycles of confining stress, so σ_3 was kept constant within each sequence. One hundred load cycles were applied per sequence at a frequency of 1 Hz. The final values of the resilient modulus (M_r) were calculated for each sequence as the average value in the last 10 cycles of the moduli obtained as follows:

$$M_r = \sigma_d/\varepsilon_r \quad (1)$$

where σ_d is the amplitude of the deviator stress, and ε_r is the recoverable strain.

Table 4. Stress levels (kPa) applied in each of the 29 sequences according to Standard UNE-EN 13286-7

Sequence	σ_3	σ_d
1	20	30
2	20	50
3	20	80
4	20	115
5	35	50
6	35	80
7	35	115
8	35	150
9	35	200
10	50	80
11	50	115
12	50	150
13	50	200
14	50	280
15	70	115
16	70	150
17	70	200
18	70	280
19	70	340
20	100	150
21	100	200
22	100	280
23	100	340
24	100	400
25	150	200
26	150	280
27	150	340
28	150	400
29	150	475

3.2. Computational modeling of resilient response

The applied stress affects the resilient behavior of granular materials more significantly than any other factor. Hence, different authors have developed constitutive laws to model the stress-strain relationship of these materials. However, the complexity of the problem made it difficult to find an equilibrium between the theoretical principles of soil mechanics and the simplicity required in procedures for routine analysis of material response [12].

The typical approach for tests with constant confining pressure continued the traditional theories of elasticity, keeping the Poisson's ratio but replacing the modulus of elasticity E by the resilient modulus M_r to take into consideration the non-linearity of the behavior (dependence of stress level). Because the resilient modulus increases with the applied stress, a large number of mathematical models were emerging over the last decades, most of them based on simple curve-fitting procedures.

One of the first models consisted of a function of the sum of the principal stresses, or bulk stress $(\theta = \sigma_1 + 2\sigma_3)$. Proposed by Hicks (1970) [33] and also known as the K-θ model, this simple hyperbolic relationship was very useful and accepted for analysis of material stiffness:

$$M_r = k_1 \cdot \theta^{k_2} \tag{2}$$

where k_1 and k_2 are material constants. However, over the following years, the model was found to simplify the stress dependency excessively because the resilient modulus is a function not only of the bulk stress but also of the magnitude of the shear strain. Thus, Uzan (1992) [34] included the deviator stress in his model:

$$M_r = k_1 \cdot \theta^{k_2} \cdot {\sigma_d}^{k_3} \tag{3}$$

Other different models have been developed until the present, taking into account other factors such as the variation of Poisson's ratio with the stress level or the effect of the density of the studied material. For this research, only one more model was considered because this model was proposed in 2004 by the National Cooperative Highway Research Program (NCHRP) [35]:

$$\frac{M_r}{P_a} = k_1 \left(\frac{\theta}{P_a}\right)^{k_2} \left(\frac{\tau_{oct}}{P_a} + 1\right)^{k_3} \tag{4}$$

where the deviator stress is replaced by the octahedral stress τ_{oct}, and P_a is a reference pressure (P_a = 101,35 kPa). Again, k_1, k_2, and k_3 are material constants.

4. Shear strength

4.1 Monotonic triaxial test

The shear strength was determined in this case by means of failure monotonic triaxial tests with a constant confining pressure (σ_3), subjecting the samples to a rising axial deviator stress (σ_d) with a constant deformation rate of 2.6% per minute (5.3 mm/min for 200 mm high and 100-mm diameter specimens) until fracture occurred. The samples were produced as in the previous section, and the internal and external pressure equalization was prevented by means of an elastic membrane. The tests were repeated with different samples over a range of different confining pressures (25 kPa, 50 kPa, 100 kPa and 200 kPa) to obtain four points of the Mohr-Coulomb envelope for each mix.

4.2 Mohr-Coulomb failure envelope

The major principal stress and deviator stress at failure, $\sigma_{1,f}$ and $\sigma_{d,f}$ (being $\sigma_{1,f} = \sigma_{d,f} + \sigma_3$) depend linearly on the confining pressure, establishing a relationship as follows [36]:

$$\sigma_{1,f} = A \cdot \sigma_3 + B \quad (5)$$

where:

$$A = (1 + \sin\varphi)/(1 - \sin\varphi) \quad (6)$$

$$B = (2C \cdot \cos\varphi)/(1 - \sin\varphi) \quad (7)$$

C is the cohesion and φ the angle of internal friction. Parameters A and B can be determined by linear regression analysis of the experimental data (array of [$\sigma_{1,f}$, σ_3]) and subsequently, C and φ can also be calculated.

Coulomb's failure criterion is represented in the Mohr diagram as a straight line that envelopes the Mohr circles obtained for different σ_3. The cohesion is also given by the intersection of the envelope with the ordinate, and φ is its slope. Thus, Coulomb's failure criterion can also be represented mathematically as [36]:

$$\tau_{ff} = \tan\varphi \cdot \sigma_{ff} + C \quad (8)$$

where τ_{ff} and σ_{ff} are the shear and normal stress in the failure plane at the failure moment.

In this case, four mixes were studied (with CDWA and NA, and cured and uncured). The water and bitumen content of the samples were chosen regarding the results of the previous dynamic triaxial test.

5. Permanent deformation behavior

5.1 Triaxial creep test

The experimental results were obtained, again, by means of dynamic triaxial tests, with sinusoidal deviator stress (σ_d) and constant confining pressure (σ_3), according to Standard UNE-EN 13286-7 [30], with 200 mm high and 100-mm diameter samples produced as described in previous sections and wrapped in elastic membranes. The tests began with the application of the initial stress σ_3 = 20 kPa and σ_d = 5 kPa (the latter was chosen to be higher than zero to assure a permanent contact between specimen and actuator). Then, up to 80,000 cycles were applied, registering the strain of 10 consecutive cycles once the following cycle number was reached: 1, 10, 50, 100, 200, 400, 1000, 2500, 5000, 7500, 10000, 12500, 15000, 20000, 30000, 40000, 50000, 60000, 70000 and 80000.

The confining pressure was kept constant at 50 kPa, but the tests were repeated with different samples and different Stress Ratios ($SR = \sigma_d/\sigma_{d,f}$), where $\sigma_{d,f} = \sigma_{1,f} - \sigma_3$ had been obtained in the previous section for each BSM-E. The SRs were selected to obtain at least five different creep curves, so that two of them remained stable until the end of the test, and other two reached the terminal *tertiary* flow stage, in which the slope of the creep curve increases again until the consequent collapse of the specimen. As in the previous case, only optimal water and bitumen content was studied, with both sorts of aggregates and before and after curing.

5.2 Computational modeling of creep response

Since the 1950s, many researchers have developed different predicting models for permanent deformation in unbound granular base layers. In the 1960s, one of the first references in this area appeared, already recommending the use of triaxial tests for this purpose [37]. Over the following decades, many developments were reported, thanks to the work of researchers such as Barksdale (1972) [38] or Francken (1977) [39]. In 1997, Huurman [23] applied Francken’s model to unbound sands and granular materials for base layers. The modification introduced by Huurman allowed the model to be dependent on the number of applied load cycles (N):

$$\varepsilon_p = A \cdot \left(\frac{N}{1000}\right)^B + C \cdot \left(e^{D \cdot \frac{N}{1000}} - 1\right) \qquad (9)$$

Huurman [23] stablished a relationship between the A, B, C and D parameters and the major principal stresses ($\sigma_1/\sigma_{1,f}$). This research line was continued by Van Niekerk (2002) [40] for base and sub-base layer materials, modifying Huurman's model to make it depend on the deviator stress ($\sigma_d/\sigma_{d,f}$).

$$A = a_1 \cdot \left(\sigma_d/\sigma_{d,f}\right)^{a_2} \qquad (10)$$

$$B = b_1 \cdot \left(\sigma_d/\sigma_{d,f}\right)^{b_2} \qquad (11)$$

$$C = c_1 \cdot \left(\sigma_d/\sigma_{d,f}\right)^{c_2} \qquad (12)$$

$$D = d_1 \cdot \left(\sigma_d/\sigma_{d,f}\right)^{d_2} \qquad (13)$$

where $\sigma_d/\sigma_{d,f}$ is the stress ratio (*SR*) that does not depend on the confining pressure (σ_3), and a_1, a_2, b_1, b_2, c_1, c_2, d_1, d_2 are material parameters. Other authors [11, 41] applied this model to stabilized materials with success, studying asphalt emulsions and foam bitumen, showing that the Huurman parameters can also be obtained for these kinds of materials.

6. Results

6.1 Resilient Modulus

Using Excel's Optimization Solver function, all model parameters were obtained by minimizing the squared error between the models and the experimental moduli obtained in the laboratory. As an example, in Figure 3, the experimental data, as well as the values of the different models, once fitted are shown for the mix with CDWA, 9% water and 6% bitumen content. Proceeding in the same way, the parameters of the five different models, as well as the regression coefficient R^2, could be determined, as Tables 5-7 show. These parameters can be used in numerical simulations to predict the resilient behavior of a certain pavement section when different loads are applied.

The results are gathered in six different levels or "steps", corresponding to the six different confining stresses (σ_3) used. Within each of these steps, the moduli also tend to increase with the variations of the deviator stress (σ_d) but in a smoother way (no steps). This stress dependence highlights the non-linear elastic behavior of these mixtures [12], similar to unbound granular materials, and confirms the hypothesis stated by Jenkins and Yu (2009) [9].

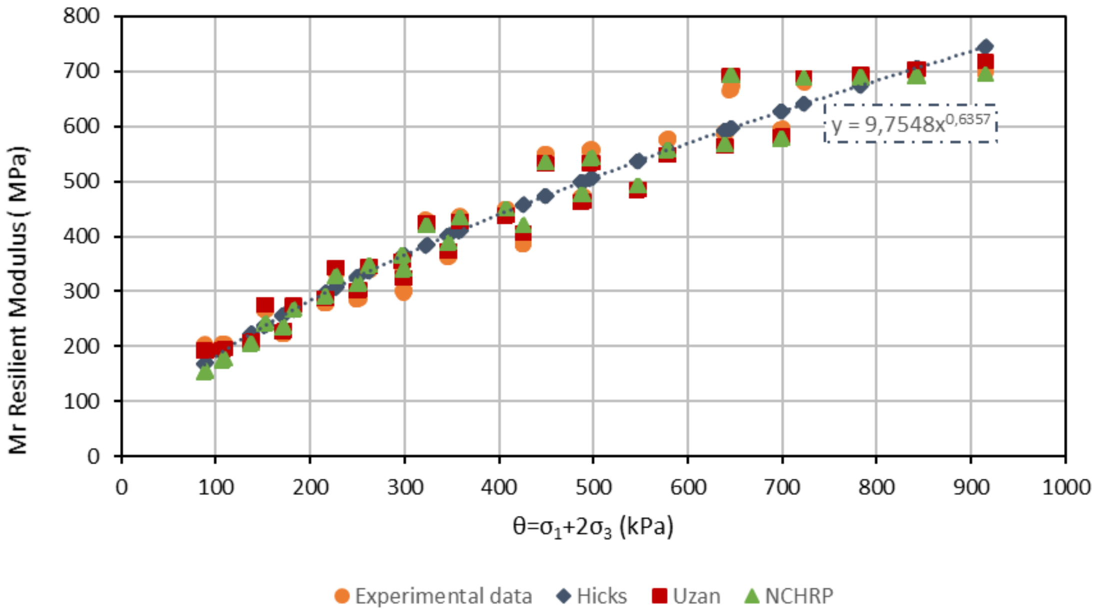

Figure 3. Fitting of Hicks', Uzan's and NCHRP models to the experimental data obtained for BSM-E with CDWA before curing with 9% water and 6% bitumen content

As Figure 3 shows, the experimental resilient modulus (M_r) was predicted very well by both the Uzan and the NCHRP models (R^2_{Uzan} = 0.9926 and R^2_{NCHRP} = 0.9857), which adopt the "step-shape" of the results very well. However, Hicks' model involves a simple interpolation through the "steps" by means of a potential curve. Hence, despite being easy to use to compare the results of different mixes, the fit to this model is poorer (R^2_{Hicks}=0.9450).

Parameters k_1, k_2 and k_3 are material constants determined by regression analyses from laboratory tests results, where k_1 is sometimes named "modulus number", k_2 is the bulk stress exponent and k_3 is an exponent determining the rate of variation of resilient modulus with σ_d. As observed by other authors in their investigation of cold asphalt mixtures with RAP [42], when adding the explicit dependence on deviator stress (regarding Uzan's against Hicks' model) into the model, k_1 decreases and k_2 increases. Parameter k_3 is always negative, which indicates that a minor stress-softening effect controlled by shear forces is superimposed on the macroscopic stress-stiffening characteristic of this kind of non-linear elastic material. These authors also found that after curing, the values of parameter k_3 became very small and, in most cases, positive. This inconsistency suggested that the use of Uzan's model may not be recommended to represent the stress-strain behavior of cold asphalt mixtures with RAP after curing. However, in the present case, this inconsistency does not happen; the present case is consistent for the both sorts of aggregate (Tables 5-6).

In Figures 4 and 5, the fitted Hicks' curves are plotted for all of the mixes studied, which easily allows a comparison among them. Mixtures with CDWA show, in general, lower stiffness than mixtures with NA, not only before the curing process but also afterwards. For instance, the resilient modulus of uncured mixes with CDWA ranked from 200 MPa to 800 MPa, while for mixes with NA, the results ranked from 200 MPa to 1000 MPa. Nevertheless, the values obtained did not become too low, being situated between the values obtained by other authors [11, 42] for similar materials, like cold-in-place recycled mixtures.

In both Figures, the curves tend to separate from each other after the curing time, showing how mixing water and bitumen content affects the results. However, before curing, the influence of the binder is practically zero, and all of the samples performed very similarly. At this point, the samples resisted the loads thanks to their mineral skeleton. Because the NA has higher mechanical quality, the specimens made with it also achieved a higher stiffness. This higher flexibility may be suitable for low/medium traffic roads where the subgrades are normally of poor quality, adjusting themselves to the deformations without cracking.

After curing the samples, it was possible to identify the optimal water and bitumen content. Mixtures with CDWA show the peak stiffness with 7%-8% bitumen content. The CDWA mix with 6% bitumen is softer for low stress but stiff for high stress. This behavior could be especially suitable for low/medium traffic roads, adapting to deformations without cracking when the loads are low (most of time in this kind of road) but resisting well in cases in which high loads might eventually damage the pavement. Furthermore, increases in the mixing water content tend to reduce the stiffness. Hence, the peak stiffness was reached with the minimum studied content (9%). As discussed in other publications [20, 21, 22], lower contents are not advisable when using CDWA because their high absorption tends to produce the premature setting of the asphalt emulsion during the mixing process, forming clots and obstructing the complete coating of the aggregates.

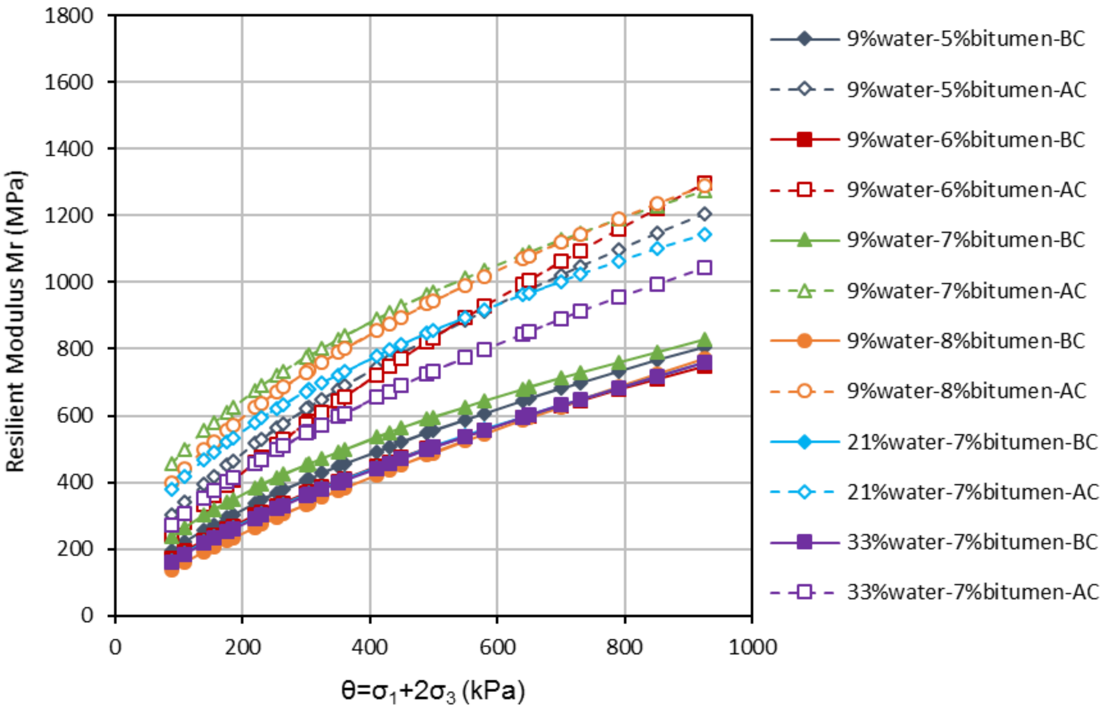

Figure 4. Representation of Hicks' model for BSM-E with CDWA before and after curing, and different water and bitumen contents

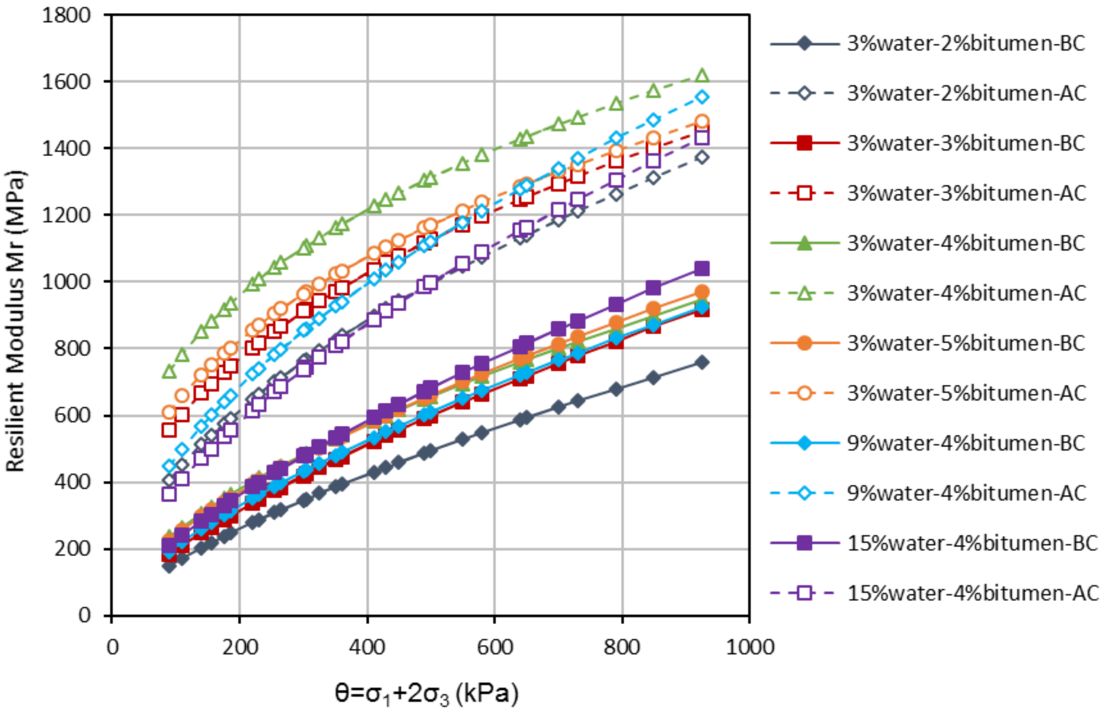

Figure 5. Representation of Hicks' model for BSM-E with NA before and after curing, and different water and bitumen contents

Table 5. Parameters of Hicks' model fitted for different mixes with CDWA and NA before and after three days curing time at 50ºC

Aggregate	% Water - %Bitumen	Before Curing			After Curing		
		k_1	k_2	R^2	k_1	k_2	R^2
Recycled Aggregate	**9%-5%**	12.829	0.606	0.842	21.266	0.591	0.972
	9%-6%	9.755	0.636	0.945	9.489	0.720	0.944
	9%-7%	21.364	0.535	0.903	62.680	0.441	0.946
	9%-8%	4.878	0.741	0.950	41.070	0.504	0.907
	21%-7%	8.637	0.655	0.946	45.276	0.473	0.870
	33%-7%	8.180	0.663	0.945	20.593	0.575	0.959
Natural Aggregate	**3%-2%**	6.574	0.695	0.947	38.846	0.522	0.938
	3%-3%	7.957	0.695	0.938	86.492	0.413	0.966
	3%-4%	16.132	0.596	0.915	157.678	0.341	0.888
	3%-5%	13.460	0.626	0.904	110.052	0.381	0.880
	9%-4%	9.337	0.673	0.939	40.865	0.533	0.955
	15%-4%	9.410	0.689	0.900	25.561	0.590	0.955

Table 6. Parameters of Uzan's model fitted for different mixes with CDWA and NA before and after three days curing time at 50ºC

Aggregate	% Water - %Bitumen	Before Curing				After Curing			
		k_1	k_2	k_3	R^2	k_1	k_2	k_3	R^2
Recycled Aggregate	**9%-5%**	7.530	1.248	-0.636	0.995	18.512	0.768	-0.188	0.995
	9%-6%	7.469	0.990	-0.355	0.993	6.998	1.113	-0.393	0.988
	9%-7%	15.474	0.958	-0.423	0.992	50.812	0.694	-0.250	0.991
	9%-8%	3.520	1.160	-0.419	0.999	29.330	0.906	-0.396	0.991
	21%-7%	6.441	1.036	-0.381	0.996	31.546	0.920	-0.444	0.988
	33%-7%	6.133	1.047	-0.385	0.996	16.625	0.846	-0.270	0.992
Natural Aggregate	**3%-2%**	4.906	1.090	-0.397	0.998	29.950	0.843	-0.319	0.993
	3%-3%	5.808	1.122	-0.430	0.998	74.484	0.604	-0.191	0.997
	3%-4%	11.583	1.033	-0.438	0.995	119.112	0.651	-0.302	0.991
	3%-5%	9.026	1.129	-0.501	0.995	82.352	0.734	-0.350	0.993
	9%-4%	6.752	1.092	-0.419	0.998	33.070	0.796	-0.262	0.991
	15%-4%	6.003	1.253	-0.562	0.998	20.162	0.902	-0.314	0.998

Table 7. Parameters of NCHRP model fitted for different mixes with CDWA and NA before and after three days curing time at 50ºC

Aggregate	% Water - %Bitumen	Before Curing				After Curing			
		k_1	k_2	k_3	R^2	k_1	k_2	k_3	R^2
Recycled Aggregate	**9%-5%**	2.142	1.104	-1.080	0.961	3.315	0.720	-0.398	0.988
	9%-6%	1.856	0.925	-0.633	0.986	2.664	1.087	-0.796	0.994
	9%-7%	2.590	0.861	-0.726	0.972	4.862	0.640	-0.447	0.983
	9%-8%	1.491	1.089	-0.738	0.993	4.336	0.847	-0.767	0.989
	21%-7%	1.799	0.984	-0.717	0.995	4.149	0.820	-0.783	0.963
	33%-7%	1.772	1.000	-0.736	0.996	2.943	0.789	-0.470	0.985
Natural Aggregate	**3%-2%**	1.639	1.012	-0.687	0.989	4.380	0.769	-0.549	0.980
	3%-3%	1.996	1.056	-0.787	0.993	5.882	0.561	-0.339	0.990
	3%-4%	2.563	0.925	-0.721	0.974	7.765	0.550	-0.477	0.950
	3%-5%	2.469	1.044	-0.911	0.986	6.582	0.653	-0.627	0.968
	9%-4%	2.103	1.018	-0.748	0.991	4.807	0.724	-0.422	0.980
	15%-4%	2.284	1.150	-0.991	0.984	3.924	0.834	-0.539	0.989

The mix with NA that reached the highest stiffness was the one with 3% mixing water and 4% bitumen content. These contents are significantly lower than those needed for BSM-E with CDWA because the absorption of NA is not, by far, so high.

Proposing as optimal mixes those with 9% mixing water and 6% residual bitumen for mixes with CDWA and 3% water and 4% bitumen for mixes with NA, the use of CDWA would involve the need for 50% extra bitumen for the construction of the same road length. However these contents refer to mix weight, and CDWA mixes are lighter than NA mixes. Therefore, to cover the same road length, the necessary mass of asphalt mix with CDWA would be lower than with NA. Making the corresponding calculations, the amount of extra bitumen was reduced to 20.2%.

6.2 Mohr-Coulomb failure envelope

Monotonic triaxial failure tests were conducted with the proposed mixes (not necessary the optimal contents for every purpose), according to the results obtained with the dynamic triaxial tests. As explained before, the proposed mix with CDWA was the mix with 9% (mixing) water and 6% (residual) bitumen content, while the optimal contents for mixes with NA were 3% water and 4% bitumen.

First, the relationship between $\sigma_{1,f}$ and σ_3 was obtained for each mix, cured and uncured (Figure 6). The major principal stress at failure ($\sigma_{1,f}$) was almost 20% higher for BSM-E with NA than with CDWA, immediately after their production. However, after being subjected to the curing process, the BSM-E with NA and BSM-E with CDWA were practically equal. Therefore, CDWA mixes are as strong as NA mixes when analyzed in the medium and long term, but they are poorer from a short-term point of view.

The σ_3 - $\sigma_{1,f}$ relationship also allowed the analytical calculation of parameters A, B and the representation of the Mohr-Coulomb diagram with four different Mohr circles (one for each confining stress) and the Coulomb's envelope. In Figure 7, an example of this calculation is represented for an uncured mix with CDWA, 9% mixing water and 6% residual bitumen. This procedure was repeated with all of the mixes. As a result, the cohesion (*C*) and angle of internal friction (φ) (Table 8) as well as the Coulomb's envelopes (Figure 8) were obtained for each mixture.

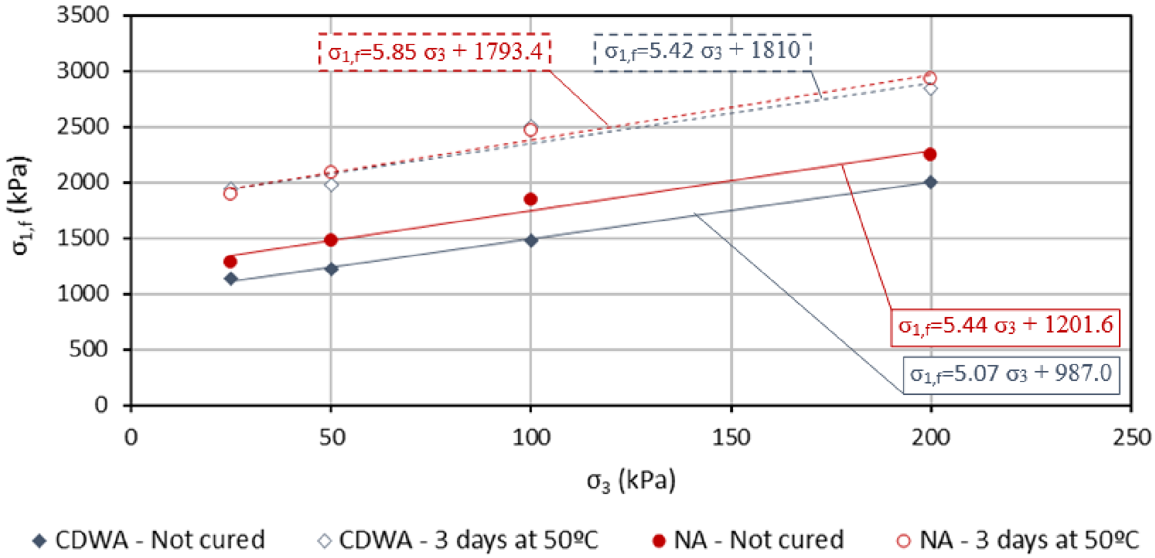

Figure 6. Relationship between the major principal stress at failure ($\sigma_{1,f}$) and the confining stress (σ_3) for cured and uncured BSM-E with CDWA and NA

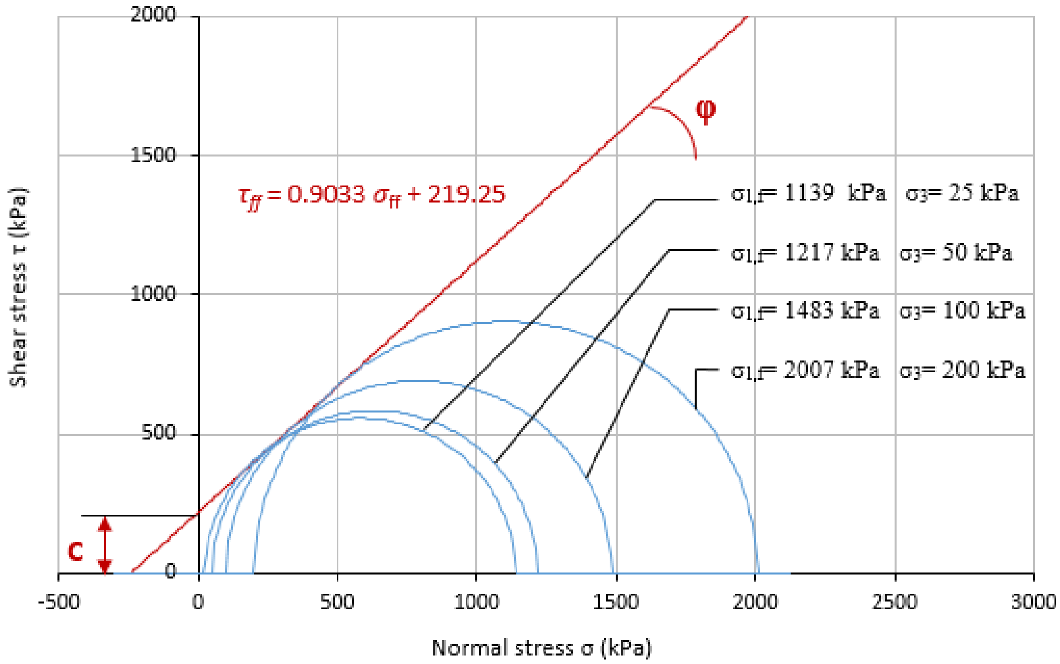

Figure 7. Example of Mohr-Coulomb diagram for uncured mixes with CDWA, 9% mixing water and 6% residual bitumen contents

Table 8. Shear parameters of the studied mixes

Aggregate	**Content (wat.–bitum.)**	**Curing**	**C (kPa)**	**φ (º)**	**R^2**
Recycled	9% - 6%	No	219.25	42.1	0.997
		3 days at 50ºC	388.71	43.5	0.939
Natural	3% - 4%	No	257.67	43.6	0.973
		3 days at 50ºC	370.68	45.1	0.981

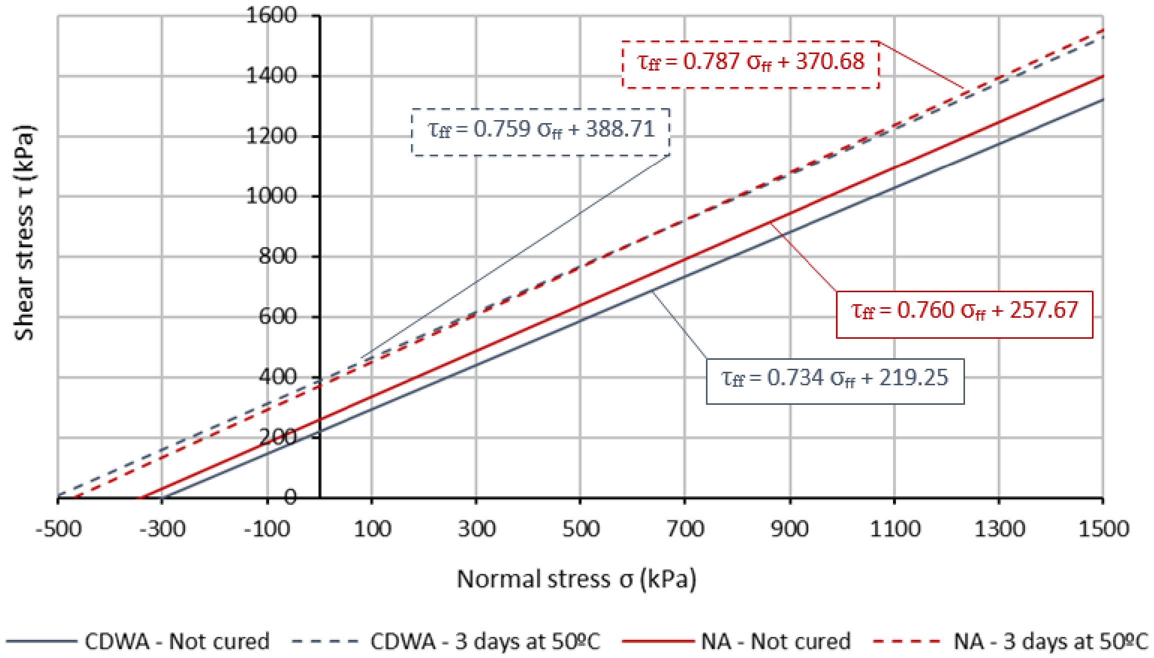

Figure 8. Mohr-Coulomb envelopes obtained for all of the mixtures studied

The cohesion is lower for BSM-E with CDWA than with NA, immediately after their production (uncured samples). However, after the curing process, their cohesion noticeably increases, reaching and even overcoming the mixes with NA.

As far as the angle of internal friction is concerned, this angle is bigger for BSM-E with NA, both before and after curing. Nevertheless, all of the registered values are similar and between 40º and 45º. The soil mechanics theory states that the failure surface can be approximated to a plane whose angle with σ_1 plane is $\theta=45^o+\varphi/2$, with φ the angle of internal friction [36]. As Figure 9 shows, the collapsed samples met this theory very well.

The values obtained are consistent and similar to those published by other authors for similar materials. For example, the cohesion of BSM-E with CDWA is similar to the value obtained by Ebels (2008) [11] for mixes with 25% RAP materials and 1% cement addition but lower than the value obtained by Dal Ben and Jenkins (2014) [43] for mixes with foam bitumen and different RAP content. The angles of internal friction are higher than those obtained by Ebels (2008) [11] and similar to the values obtained by Dal Ben and Jenkins (2014) [43] with foam bitumen and 0% of RAP content.

Figure 9. Appearance of a sample after failure by monotonic triaxial tests, with the failure plane at approximately 66º. Example with CDWA uncured mix (φ = 42.1º)

6.3 Permanent deformation

Once obtained, the relationship $\sigma_{1,f}$ - σ_3 in the previous section, showed that the values of $\sigma_{1,\mathrm{f}}$ and $\sigma_{d,f}$ could be calculated directly by fixing the test confining pressure to 50 kPa. These values can be seen in Table 9. The Stress Ratio (SR = σ_d /$\sigma_{d,f}$) applied in each test would be based on these values.

For each mix, the creep curves like those presented as an example in Figure 10 were plotted. At least five curves were obtained with different SR values. In this case, the critical SR that produces the appearance of the tertiary flow stage and the collapse of the sample before reaching 80,000 cycles was 40%. For the rest of the mixtures, the results are summarized in Table 10. The critical SR is higher for uncured BSM-E with CDWA (60%) than with NA (50%) but after curing, both mixes showed the same critical SR (40%). Thus, with the curing time, the critical SR tends to decrease. Moreover, in absolute terms, the deviator stress necessary to produce the failure of the samples is higher for BSM-E with CDWA and higher again for cured mixes (logically). Therefore, BSM-E with CDWA not only resisted loads closer to their failure stress (higher SR) but also resisted higher major principal stress in absolute terms.

Huurman parameters (*A*, *B*, *C* and *D*) were obtained by using Excel's Optimization Solver function, fitting the model to the creep curves until the minimum squared error was reached. All of the curves can be seen in Table 11. In general terms, the curves tend to increase with the SR. When the tertiary flow stage is not reached, C and D values are zero, and Huurman's model is consists only of the first term, depending only on parameters A and B. Parameters a_1, a_2, b_1, b_2, c_1, c_2, d_1, d_2 are summarized in Table 12 because they are useful for further numerical simulations. The fitting of parameters c_1, c_2, d_1, d_2 could be done only when C and D were different from zero. For each mix, only two or three data points were available, which might reduce the quality of their fit.

Table 9. Major principal stress and deviator stress at failure for σ_3 = 50 kPa

Mix	$\sigma_{1,f}$ (kPa)	$\sigma_{d,f}$ (kPa)	σ_3 (kPa)
CDWA – Not cured	1240	1190	50
CDWA - Cured	2081	2031	50
NA – Not cured	1473	1423	50
NA - Cured	2086	2036	50

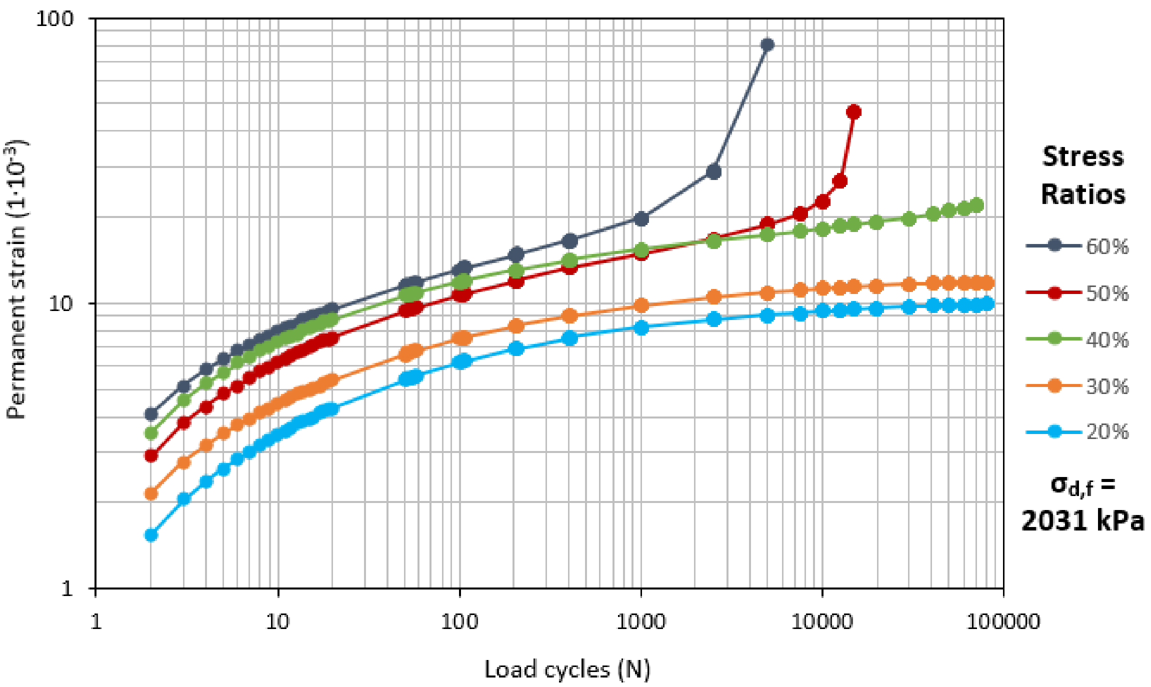

Figure 10. Example of creep curves obtained with five different stress ratios for the mix with CDWA, 9% mixing water and 6% residual bitumen, after three days of curing at 50ºC

Table 10. Critical principal stresses that produced the appearance of the tertiary flow stage and the failure of the samples before 80,000 load cycles

Mix	$\sigma_{d,f}$ (kPa)	$\sigma_{d,a}$ (kPa)	SR	σ_3 (kPa)
CDWA – Not cured	1190	714	60%	50
CDWA - Cured	2031	812	40%	50
NA – Not cured	1423	712	50%	50
NA - Cured	2036	814	40%	50

Table 11. Huurman's parameters (A, B, C, D) for the studied BSM-E as a function of SR

Stress Ratio	A	B	C	D	R^2
CDWA mix – not cured					
30%	9.925	0.026	0	0	0.962
40%	9.670	0.026	0	0	0.962
50%	14.053	0.045	0	0	0.971
60%	17.123	0.179	0.0071	0.045263	0.982
70%	19.573	0.205	0.000202	4.236339	0.998
CDWA mix – cured for three days at 50ºC					
20%	8.466	0.039	0	0	0.964
30%	10.122	0.040	0	0	0.947
40%	15.349	0.073	0.008	0.066	0.998
50%	14.599	0.166	0.008275	0.530835	0.996
60%	19.781	0.388	0.009073	1.693143	1.000
NA mix – not cured					
20%	8.529	0.025	0	0	0.999
30%	9.318	0.034	0	0	0.994
40%	13.493	0.046	0	0	0.965
50%	16.599	0.292	0.008461	0.381770	0.997
60%	23.978	0.274	0.248373	3.942603	1.000
NA mix – cured for three days at 50ºC					
20%	9.988	0.033	0	0	0.956
30%	14.490	0.059	0	0	0.983
40%	16.208	0.143	0.007356	0.137838	0.999
50%	18.613	0.287	0.005236	1.698305	1.000
60%	22.420	0.224	0.007291	5.940463	1.000

Table 12. Parameters of the relationship between Huurman's parameters (A, B, C, D) and SR

	a_1	a_2	b_1	b_2	c_1	c_2	d_1	d_2
CDWA-Not cured	0.4261	0.8936	0.000001	2.7873	$1 \cdot 10^{-21}$	9.7506	$9 \cdot 10^{-46}$	24.703
CDWA- Cured	0.8552	0.7533	0.00005	2.0674	$5 \cdot 10^{-19}$	9.4728	$2 \cdot 10^{-19}$	10.784
NA-Not cured	0.4606	0.9308	0.00001	2.4538	$1 \cdot 10^{-35}$	19.303	$1 \cdot 10^{-36}$	20.649
CDWA-Cured	1.2902	0.692	0.00007	2.0299	$7 \cdot 10^{-13}$	5.7974	$1 \cdot 10^{-27}$	15.854

7. Conclusions

In the present paper, the resilient modulus (M_r) as well as the Mohr-Coulomb envelopes and the permanent deformation were obtained experimentally, and different predicting models were fitted to the data, which may be a useful tool in future investigations, for example, for numerical simulations of the behavior of BSM-E with CDWA. So far, some conclusions can already be reached, as listed below:

1. Dynamic triaxial tests with BSM-E showed a clear dependence of their behavior on both major (σ_1) and minor (σ_3) principal stress, highlighting their non-linear elastic nature. The dependence is greater on confining stresses than on deviator stress.

2. Hicks' model is easy to use to compare the non-linear elastic behavior of different mixtures at a glance. However, the fit is considerably better with Uzan's and NCHRP models, which are more accurate to numerically model the performance of BSM-E.

3. The influence of the fresh binder on the resilient modulus of the specimens before curing is practically zero. Hence, all of the samples performed very similarly, no matter how much the bitumen content was varied, even though BSM-E with CDWA is more flexible than mixes with NA not only before but also after curing processes. The major influence of the mineral skeleton is stronger for the case of NA. Nevertheless, the results are not excessively low because they are situated between the results obtained by other authors with similar mixtures and without CDWA. This behavior may be especially suitable for flexible pavements in low/medium traffic roads in which the subgrades are normally of poor quality because they can adjust themselves to the deformations without cracking.

4. Before the curing process, BSM-E with CDWA showed lower cohesion and resisted lower deviator stress at failure than mixes with NA. However, after curing, mixes with both kinds of aggregate reached practically the same strength.

5. In general, mixes with CDWA provided better creep behavior. They not only resisted loads closer to their respective failure loads but also resisted loads that were higher in absolute terms without reaching the tertiary flow creep stage and the consequent failure of the specimens.

6. Despite showing good mechanical performance, BSM-E with CDWA needed higher water and bitumen content. Thus, the proposed mixes were those with 9% mixing water and 6% residual bitumen for mixes with CDWA and 3% water and 4% bitumen for mixes with NA, requiring 20.2% extra bitumen for the construction of the same length of road.

Acknowledgements

The authors would like to acknowledge the funding of the project BIA2010-17751 and the scholarship FPI (ref. BES-2011-044377) from the Spanish Ministry of Economy and Competitiveness. The authors also would like to express their sincere gratitude to the GESTAN Group for the CDWA and to ECOASFALT for the bitumen emulsion generously donated for the present research.

References

[1] Thanaya INA, Zoorob SE, Forth JP. A laboratory study on cold-mix, cold lay emulsion mixtures. Proc Inst Civ Eng Transp 2009;162:47–55.

[2] Nageim H, Al-Busaltan SF, Atherton W, Sharples G. A comparative study for improving the mechanical properties of cold bituminous emulsion mixtures with cement and waste materials. Constr Build Mater 2012;36:743–8.

[3] Read J, Whiteoak D. The shell bitumen handbook. London: Thomas Telford Publishing; 2003.

[4] HAUC (Highway Authority and Utility Committee). Specification for the reinstatement of opening in highways. new roads and street works. In: Act 1991. London. UK: HMSO; 1992.

[5] James A. Overview of asphalt emulsions. Asphalt emulsion technology, transportation research circular number E-C102. Washington DC (USA): Transportation Research Board; 2006

[6] Oruc S, Celik F, Akpinar MV. Effect of Cement on Emulsified Asphalt Mixtures. J Mater Eng Perform 2007;16(5):578-83.

[7] Oruc S. Neural network model for temperature sensitivity of emulsified asphalt mixtures. Indian J Eng Mater Sci 2010;17(6):438-48.

[8] Chu H, Zhang J, Lu YH. Experimental study on pavement performance of emulsified asphalt cement concrete. Appl Mech Mater 2013;357-360:888-92.

[9] Jenkins KH, Yu M. Cold-recycling techniques using bitumen stabilization: Where is this technology going? ASCE Geotechnical Special Publication 2009:191–200.

[10] Jenkins KH, Long FM, Ebels LJ. Foamed bitumen mixes=shear performance? Int J Pavement Eng 2007;8(2):85–98.

[11] Ebels LJ. Characterisation of material properties and behavior of cold bituminous mixtures for road pavements. Stellenbosh University (South Africa): Doctoral Dissertation; 2008.

[12] Lekarp F, Isacsson U, Dawson A. State of the art. I: Resilient response of unbound aggregates. J Transportation Eng 2000;126(1):66-75.

[13] Yun T, Kim YR. Viscoelastoplastic modeling of the behavior of hot mix asphalt in compression. KSCE J Civ Eng 2013;17(6):1323-32

[14] González-Fonteboa B, Martínez-Abella F. Shear strength of recycled concrete beams. Constr Build Mater 2007;21:887-893.

[15] Limbachiya M, Meddah MS, Ouchagour Y. Use of recycled concrete aggregate in fly-ash concrete. Constr Build Mater 2012;27:439-449.

[16] Pepe M, Toledo Filho RD, Koenders EAB, Martinelli E. Alternative processing procedures for recycled aggregates in structural concrete. Constr Build Mater 2014;69:124-132.

[17] Wong YD, Sun DD, Lai D Value-added utilization of recycled concrete in hot-mix asphalt. Waste Manag 2007;27:294-301.

[18] Pérez I, Pasandín AR, Medina L. Hot mix asphalt using C&D waste as coarse aggregates. Mater Des 2012;36:849-846.

[19] Pasandín AR, Pérez I. Overview of bituminous mixtures made with recycled concrete aggregates. Constr Build Mater 2015;74:151-161.

[20] Gómez-Meijide B, Pérez I. A proposed methodology for the global study of the mechanical properties of cold asphalt mixtures. Mater Des 2014;57:520–7.

[21] Gómez-Meijide B, Pérez I. Effects of the use of construction and demolition waste aggregates in cold asphalt mixtures. Constr Build Mater 2014;51:267–77.

[22] Gómez-Meijide B, Pérez I, Airey G, Thom N. Stiffness of cold asphalt mixtures with recycled aggregates from construction and demolition waste. Constr Build Mater 2015;77:168–78.

[23] Huurman H. Permanent deformation in concrete block pavements. Delft University of Technology (The Netherlands): Doctoral Dissertation; 1997.

[24] AENOR (Asociación Española de Normalización y Certificación). UNE EN 933–3. Ensayos para determinar las propiedades geométricas de los áridos. Parte 3: Determinación de la forma de las partículas. Índice de lajas. Madrid (Spain): AENOR; 2012.

[25] AENOR (Asociación Española de Normalización y Certificación). UNE EN 933–5. Ensayos para determinar las propiedades geométricas de los áridos. Parte 5: Determinación del porcentaje de caras de fractura de las partículas de árido grueso. Madrid (Spain): AENOR; 1999.

[26] AENOR (Asociación Española de Normalización y Certificación). UNE EN 933– 8. Ensayos para determinar las propiedades geométricas de los áridos. Parte 8: Evaluación de los finos. Ensayo del equivalente de arena. Madrid (Spain): AENOR; 2000.

[27] AENOR (Asociación Española de Normalización y Certificación). UNE EN 1097– 2. Ensayos para determinar las propiedades mecánicas y físicas de los áridos. Parte 2: Métodos para la determinación de la resistencia a la fragmentación. Madrid (Spain): AENOR; 2010.

[28] AENOR (Asociación Española de Normalización y Certificación). UNE EN 1097– 6. Ensayos para determinar las propiedades mecánicas y físicas de los áridos. Parte 6: Determinación de la densidad de partículas y la absorción de agua. Madrid (Spain): AENOR; 2006.

[29] ATEB (Technical Association of Bituminous Emulsions). Gravel-emulsion specifications. ATEB (consulted on-line in <http://www.ateb.es/pdf/PLI_GRAVA.pdf> last time on 29/05/2015).

[30] AENOR (Asociación Española de Normalización y Certificación). UNE-EN 13286-7:2008. Mezclas de áridos sin ligante y con conglomerante hidráulico. Parte 7: Ensayo triaxial con carga cíclica para mezclas sin ligante. Madrid (Spain): AENOR; 2008.

[31] Association Française de Normalisation. Norme Française NFP 98-251-1. Enrobés hydrocarbonés. Essais statiques sur mélanges hydrocarbonés. partie1: Essais Duriez sur mélanges hydrocarbonés à chaud. Paris (France); 2004.

[32] Kim W, Labuz JF. Resilient modulus and strength of base course with recycled bituminous material. University of Minnesota (USA): Technical report; 2007.

[33] Hicks RG. Factors influencing the resilient response of granular materials. University of California, Berkeley (USA): Doctoral Dissertation; 1970.

[34] Uzan J, Witczak MW, Scullion T, Lytton RL. Development and validation of realistic pavement response models. Proceedings of the 7th International Conference on Asphalt Pavements. Nottingham (UK); 1992.

[35] NCHRP (National Cooperative Highway Research Program). Guide for Mechanistic-Empirical Design of New and Rehabilitated Pavement Structures. Part 2. Design Inputs. Final Report NCHRP 1-37A; 2004.

[36] Lambe TW, Whitman RV. Soil Mechanics. USA: John Wiley & Sons; 1969.

[37] Haynes JH, Yoder EJ. Effects of repeated loading on gravel and crushed stone base course materials. Highw Res Rec: J Highw Res Board 39. Washington (USA); 1962.

[38] Barksdale RD. Laboratory evaluation of rutting in base course materials. 3rd International Conference on the Structural Design of Asphalt Pavements. London (UK); 1972.

[39] Francken L. Permanent deformation law of bituminous road mixes in repeated triaxial compression. 4th International Conference on the Structural Design of asphalt Pavements. Ann Arbor. Michigan. USA; 1977.

[40] Van Niekerk AA. Mechanical behavior and performance of granular bases and sub-bases in pavements. Delft University of Technology (The Netherlands): Doctoral Dissertation; 2002.

[41] Jenkins KH. Mix design considerations for cold and half-warm bituminous mixes with emphasis on foamed bitumen. University of Stellenbosh (South Africa): Doctoral Dissertation; 2000.

[42] Santagata E, Chiappinelli G, Riviera PP, Baglieri O. Triaxial testing for the short term evaluation of cold-recycled bituminous mixtures. Asph Pavements Environ 2010;11(1):123-147.

[43] Dal Ben M, Jenkins KJ. Performance of cold recycling materials with foamed bitumen and increasing percentage of reclaimed asphalt pavement. Road Mater Pavement Des 2014;15(2):348-371.